Martin BLAVIER[1]
[1]Theoretical Physical Chemistry, UR MOLSYS,
University of Liège, 4000 Liège, Belgium
*Phone Number: +32 494 26 99 65,
Email Address: martin.blavier@uliege.be,
Present address: NANOCHEM, UR MOLSYS,
University of Liège, 4000 Liège, Belgium

Investigation of Ultrafast Phenomena in Attochemistry using Singular Value Decomposition

The following article describes results in the field of (theoretical) attochemistry, a recent discipline focused on the effects of ultrafast (less than a femtosecond) optical pulses on molecular systems and the discovery of potentially new and exotic reaction pathways. This discipline would not have appeared without the creation of the field of attosecond physics, whose breakthroughs allowed the understanding and the creation of such ultrafast optical pulses. Attosecond physics have recently made the news, as this year Pierre Agostini, Ferenc Krausz and Anne L'Huillier were award the Nobel Prize in Physics "for experimental methods that generate attosecond pulses of light for the study of electron dynamics in matter". [1] In that regard, this article proves to be in the spirit of the times.

Abstract
In attochemistry, attopulses are used to initiate chemical reactions. The intrinsically coherent molecular dynamics which arises from the interaction of matter with ultrashort pulses might lead to new synthetic possibilities. The experimental study of attochemical phenomena is, however, a difficult task which relies on theoretical models to obtain insights in the effects at play. These theoretical models are nevertheless also difficult to set up and the subsequent analysis of the data is rarely straightforward. Therefore, any method that might simplify the creation of a suitable theoretical model of a system or the analysis of the data produced is useful. In this article, one such method, the singular value decomposition, is considered. The handiness of this decomposition is then exemplified with two different examples: the study of the isotope effect in the Jahn-Teller rearrangement of the methane cation and the analysis of the evolution of the entanglement in the photoexcitation of lithium hydride.
Keywords: Attochemistry, Singular Value Decomposition, Entanglement, Molecular Quantum Dynamics

[1] *The Nobel Prize in Physics 2023*. NobelPrize.org. https://www.nobelprize.org/prizes/physics/2023/press-release/ (accessed 2023-11-07).

https://doi.org/10.52809/cn2023/SGJI2324

1. Introduction

Along with the familiar paradigm of thermal chemistry, another most common activation method is photochemistry, where the energy used to activate chemical bonds and induce chemical reactions arises from electromagnetic radiations. The history of photochemistry begins long before the idea of chemistry and even mankind first appeared, displaying crucial roles in the early synthesis of organic compounds or in complex biological reactions such as photosynthesis. But photochemistry proves to be important for more than those natural examples and display an accrued interest for its synthetic possibilities [1].

On a fundamental point of view, even more promising possibilities have been made available recently due to advances in attosecond science [2], opening the door for the emergence of the field of attochemistry. In attochemistry, ultrashort optical pulses are used to excite specifically electronic motion before the onset of nuclear motion, allowing for the observation and possibly the control of the electronic density on its own time scale, the attoscale (10^{-18} – 10^{-15} s) [3-6].

Because of their extremely short duration, attopulses are characterized by a broad energy bandwidth, which can be resonant with several electronic states of a molecule, leading to the formation of a coherent superposition of electronic states in the initial state of the quantum dynamics. These intrinsically coherent electronic dynamics on a superposition of electronic states are an essential feature of attochemistry, separating it with the closely related field of femtochemistry [7], in which a single electronic state is populated and the electronic dynamics only show a coherent character when electronic states are close in energy (for example near avoided crossings or conical intersections) and not from their very beginning. This difference in dynamics might provide an access to new chemical reactions, allowing either to obtain new compounds or discover new pathways to create already known ones. These newfound synthetic possibilities show much promise for attochemistry.

Attochemical experiments are nevertheless burdened by the inherent complexity of the data obtained, in part due to the coherent character of the dynamics. The accurate and comprehensive interpretation of the results remains a heavy task and, in many cases, a theoretical model of the underlying molecular quantum dynamics is necessary to provide insights to the experimental data.

The setting up these theoretical models is nevertheless no bed of roses, as the highly coherent dynamics exhibited in attochemistry require a suitable description of electronic coherences, that is, interference effects between several electronic states. In this article, the molecular dynamics of the system considered were computed using a fully quantum method, which allows for a full description of the electronic coherences. However, this method proves to be computationally intensive for all systems, even small molecules like CH_4, as it suffers from the curse of dimensionality [8]: the computational cost scales exponentially with the number of degrees of freedom in the system. Here, the degrees of freedom considered are of vibrational and electronic nature.

This high computational cost thus motivates the use of algebraic methods to either decrease the complexity of the quantum computations or to allow a simpler or different insight into the large amount of data obtained from the theoretical models might prove invaluable. One such algebraic method is investigated here: the singular value decomposition (SVD). The SVD is an algebraic decomposition widely used in statistics and genomics to either decouple in a given matrix two degrees of freedom of different nature or to extract the best few-rank approximation of this matrix. Those two approaches prove to be of interest for the study of attochemical phenomena, as it will be exemplified for **two different applications**: first by the study of the isotope effect in the ultrafast Jahn-Teller rearrangement of the methane cation (CH_4^+) and then by the study of the evolution of the entanglement in the photoexcitation of lithium hydride (LiH). These

two systems were described on a grid of nuclear geometries in order to compute their quantum dynamics.

This article will first consist of a theoretical review of the concepts behind molecular quantum dynamics on a grid and the singular value decomposition, followed by a short description of the results obtained through these techniques on the molecules of interest.

Box 1. Coherent Dynamics

A quintessential feature of quantum mechanics is the superposition principle, which states that given two states of a system, the sum (superposition) of the two states gives another valid state for the system of interest. The probability density given by the square modulus of such resulting state is then more complex than simply the (weighted) sum of the probability density for each state, and interference effects appear. These interference effects also impact the time evolution of the resulting state, as it cannot be an eigenstate of the Hamiltonian operator. [9]

In quantum chemistry, the electrons are described using electronic states, which are the eigenstates of the electronic Hamiltonian operator [10]. By the superposition principle, a sum of several electronic states is another valid initial state for the electronic motion, but the probability density for the resulting state and its time evolution will display interference effects between one electronic state and another, resulting in so-called coherent ("interfering") dynamics between electronic states. This coherent superposition of electronic states can be produced either directly by the photoexcitation of a molecule with a large energy-bandwidth optical pulse, such as an attopulse, or during the molecular dynamics through non-adiabatic couplings, which will be discussed later.

2. Theory

2.1. Quantum molecular dynamics on a grid

In order to describe the quantum dynamics of the molecular systems we wish to study, we must solve numerically the Time Dependent Schrödinger Equation (TDSE) .

$$i\hbar\frac{\partial\psi}{\partial t} = \hat{H}(t)\psi,\ \ \psi(t_0) = \psi_0 \qquad 1.1.$$

Two important quantities must be provided in the previous equation: the Hamiltonian operator associated with the system $\hat{H}(t)$ and the initial state of the system Ψ_o. To this end, the possible states of the system (three coordinates for each electron and each nucleus in the molecule) must be discretized. In order to simplify the computations, the Born-Oppenheimer approximation is used, an approximation which considers that one can decouple the motion of the electrons and the nuclei because of their difference in mass for each geometry of the nuclei. This approximation allows the computation of adiabatic electronic potentials for the molecule. These potentials, along with the Coulomb repulsion of the nuclei, constitute effective potentials in which the nuclei move.

This leads to a considerable reduction in the degrees of freedom to take into account in the molecular dynamics, as the electronic degrees of freedom are decoupled from the nuclear ones. However, this decoupling is approximate since the electronic states resulting from the BO approximation are coupled by non-adiabatic interactions driven by the nuclear motion (see below), and the number of coupled electronic states can be large as the dynamics unfolds. Moreover, this is not sufficient, as the discrete description of the remaining nuclear degrees of freedom scales exponentially with the number of nuclear coordinates to account for. Currently, grid-based molecular dynamics on several coupled electronic states involving more than three nuclear coordinates prove to be intractable. In the case of non-linear molecules, this leads therefore to the need of reducing the dimensionality of the problem even further by

restricting the model to the appropriate nuclear coordinates for the description of the dynamics.

Only then can we begin to describe the state space of the system as a grid of several orthogonal grid points, representing each a different nuclear geometry and to which different electronic states are associated. The wavefunction of the system will thus be described as sum of product terms made of a complex amplitude associated with each grid point and each electronic state, amplitude denoted c_{gi}. The set of all these amplitudes then consists of an amplitude vector c. This is represented visually in figure 1, which shows the grid points which are coupled due to the non locality of the kinetic energy and momentum operators represented in a finite difference approximation for two nuclear coordinates [11]. The structure of the kinetic energy and momentum operator in the system of coordinates used in [11] is also depicted.

The choice of this basis for the nuclear wavefunction allows us to express the nuclear Hamiltonian operator which will act on the amplitude vector in a matrix form. Its elements are given by expression (1.2)

$$= \mathbf{V}_{gi,g'j}\delta_{gg'}\delta_{ij} + (\mathbf{T}_N)_{gi,g'j}\delta_{ij} \\ g)\delta_{gg'})(\mathbf{p}_{gi,g'j}\delta_{ij}) - (\mu_{ij}(g)\delta_{gg'}) \cdot \mathbf{E}(t) \quad 1.2.$$

In equation (1.2), $V_{gi,g'j}\ \delta_{g'}\ \delta_{ij}$ is the potential energy operator of the system, which is given as the potential energy surface of a given electronic state at a given grid point. This operator is both diagonal on the grid and on the electronic states.

T_N is the nuclear kinetic energy operator, which is represented in figure 1. for a grid of two nuclear coordinates. The μ are the reduced masses of the system according to the different coordinates considered. This operator does not act on the adiabatic electronic states and thus is diagonal on the electronic states. The nonlocal character of the second order derivative with respect to the nuclear coordinate is approximated as finite differences on the grid, allowing for a numerical resolution of the TDSE [12].

In Eq. (1.2), $\tau_{ij}(g)$ are the derivative couplings between two different electronic states at a given grid point. They are given by electronic structure computations and diagonal on the grid. Along

$$T_N = \frac{1}{\mu_1}\frac{\partial^2}{\partial q_1^2} + \frac{1}{\mu_2}\frac{\partial^2}{\partial q_2^2} + \frac{1}{\mu_{12}}\frac{\partial^2}{\partial q_1 \partial q_2} \qquad \mathbf{p} = -i\hbar\left(\frac{\partial}{\partial q_1}, \frac{\partial}{\partial q_2}\right)$$

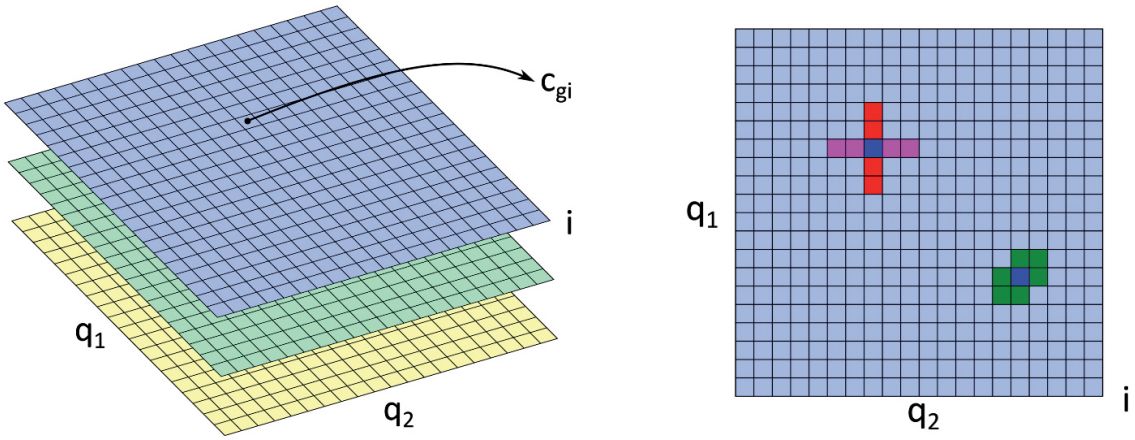

Figure 1: Grid description of the molecular system for the dynamics. q_1 and q_2 are two different nuclear coordinates, whereas the plane i describes the i-th electronic state. On the right, the structure of the kinetic energy and momentum operator on the grid are represented in the framework of finite differences [11, 12].

with the momentum operator $P_{gi,g'j}$, they describe non-adiabatic couplings between the electronic states which result from a breakdown of Born-Oppenheimer approximation. The momentum operator $P_{gi,g'j}$ is similar in structure to the nuclear kinetic energy term as it is diagonal on the electronic states and the nonlocal property of its first derivative is also approximated using finite differences. It is also represented in figure 1 for a grid of two nuclear coordinates.

The non-adiabatic couplings described by the derivative couplings and the momentum operator arise from the coupling of the motion of the electrons and the nuclei and essentially represent a breakdown of the Born-Oppenheimer approximation. These couplings are the strongest when different electronic potentials are close in energy. They play a crucial role in photochemistry, as it will be shown in the study of the methane cation and the photoexcitation of LiH.

Box 2. Non-adiabaticity

The Born-Oppenheimer approximation allows to decouple the motion of the electron and the nuclei in a molecule. This approximation is motivated by the larger mass of the nuclei compared to the electrons, leading to different time scales for their respective motions and to adiabaticity (decoupling between the motion of the light particles and the heavy particles). It was initially devised by Max Born and J. Robert Oppenheimer [13] to describe the ground state of molecules, which is most of the time well-separated in energy from the excited electronic states and for which this approximation is justified. However, it breaks down as soon as the spacing between several electronic states become close to the spacing between vibrational states, that is, when a coupling between electronic and nuclear motions becomes possible [14]. This is especially the case near conical intersections, where two or more adiabatic electronic states cross, or avoided crossings, if the electronic states do not ultimately cross but are in close vicinity. These non-adiabatic, or vibronic, couplings lead to the transfer of amplitudes between several electronic states, thereby adding complexity to the quantum dynamics and possibly changing the coherent superposition of the electronic states.

Finally, the interaction with the electric field of an exciting pulse depends on both the permanent $\mu_{ii,}(g)$ and transition $\mu_{ii,}(g)$ dipole moments for the electronic states, which are also given by electronic structure computations at a given grid point, and thus which are diagonal on the grid. In the case of the photoexcitation of , the electric field of the exciting pulse is described by equation (1.3). It is modelled by a Gaussian envelope centred around t_o with a standard deviation specifying the length of the pulse. The carrier frequency of the pulse is given by ω and the carrier-envelope phase (CEP) is ϕ. The maximal amplitude of the pulse is given by $|E_o|$. The term $-\frac{sin(\omega t+\phi)(t-t_o)}{\omega\sigma^2}$ is present in the expression of the pulse to ensure that it remains Fourier-limited even for few-cycle pulses [15].

Thanks to the diagonal character of many operators involved in the Hamiltonian matrix as well as the use of finite difference approximations for the first and the second derivatives with respect to nuclear coordinates, a lot of elements of the Hamiltonian matrix (1.2) are zero and the Hamiltonian matrix is referred to as a “sparse” matrix. The several common linear algebra operations, such as matrix-vector multiplication, can be tailored to take advantage of the sparse structure of the matrix and perform more efficiently the desired operation.

$$\mathbf{E}(t) = |\mathbf{E}_0|\hat{\mathbf{e}}\, exp\left(-\frac{(t-t_0)^2}{2\sigma^2}\right)\left(cos(\omega t+\phi) - \frac{sin(\omega t+\phi)\,(t-t_0)}{\omega\sigma^2}\right) \quad 1.3.$$

In the case of the propagation of the TDSE (1.1), the nuclear wavefunction is written as a vector of coefficients c_{gi} on the grid, and matrix-vector multiplication of the Hamiltonian matrix (1.2) on the wave vector is performed.

In order to compute the quantum dynamics of the molecular system, we still require an initial state. The choice of this initial state will depend on the phenomenon that is under study. In the first example we will describe, our interest lies in the study of the dynamics occurring in the methane cation produced by high-harmonic spectroscopy (HHS) [16]. This leads us to compute the initial states that arise in HHS. In the second example, the study of the entanglement in the photoexcitation of LiH, the initial state was chosen to be the lowest vibrational state of the ground electronic state. This choice is sensible as the lowest vibrational state is the only populated state in this molecule at room temperature.

The TDSE (1.1) is then numerically integrated at each time step using the Hamiltonian matrix and the initial state previously described in order to express the time evolution of the system. A numerical integration is here necessary as the molecular Hamiltonian, containing the interaction with a time-dependent optical pulse, is time-dependent. This integration is carried out using a fourth-order Runge-Kutta procedure, widely used for solving numerically first-order differential equations.

2.2. Singular value decomposition

The singular value decomposition (SVD) is an algebraic decomposition of matrices with important applications in statistics, signal processing and genomics [17-20]. The importance of this decomposition arises from its universality: all matrices, especially rectangular ones, can be decomposed by SVD.

Mathematically ([21]), let A be a rectangular complex-valued matrix of dimensions $M \times N$, with $M > N$ (the case would simply produce the adjoint of the following expressions). Then this matrix admits a decomposition in the form (the notation $V^\dagger$; means taking the Hermitian conjugate of the matrix V):

$$\mathbf{A} = \mathbf{U\Sigma V}^\dagger \qquad 1.4.$$

With U a rectangular $M \times N$ matrix whose columns are the *left singular vectors* of A, that is the normalized eigenvectors corresponding to the non-zero eigenvalues of the square matrix $AA^\dagger$; Σ the square $M \times N$ matrix containing the *singular values* of A, that is the square roots of the non-zero eigenvalues of both $AA^\dagger$ and $A^\dagger A$ (which importantly have the same eigenvalues but different eigenvectors); V the square $M \times N$ matrix whose columns are the *right singular vectors* of A, *i.e.* the normalized eigenvectors of the non-zero eigenvalues of $A^\dagger A$. In most cases, the singular vectors are complex-valued, whereas the singular values are always real. This decomposition is called the (compact) singular value decomposition of A.

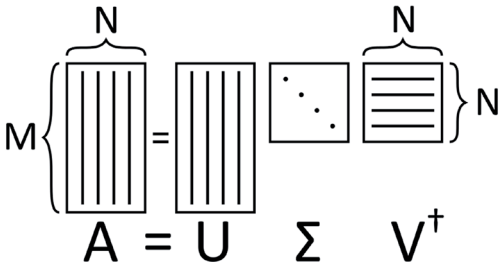

Figure 2: Illustration of the singular value decomposition

The SVD also allows to express the matrix A as a sum of rank-one matrices $u_i v_i^\dagger$:

$$\mathbf{A} = \sigma_1 \mathbf{u}_1 \mathbf{v}_1^\dagger + \sigma_2 \mathbf{u}_2 \mathbf{v}_2^\dagger + \sigma_3 \mathbf{u}_3 \mathbf{v}_3^\dagger + \cdots = \sum_{i=1} \sigma_i \mathbf{u}_i \mathbf{v}_i^\dagger \quad 1.5.$$

With $R \leq N$ the rank of A. The singular values are given in decreasing order in expression (1.5). If we stop the sum in this expression at a given rank R', the matrix obtained constitutes the best rank R' approximation of A. This provides with a way to reduce efficiently the rank of a matrix in the hope of simplifying the subsequent computations using that matrix. The first elements of this decomposition describe the broad features of the original matrix A, whereas the last elements of the series describe extremely localized features. By analogy with the

application of SVD to images, we can say that the terms associated with the greatest singular values represent low frequency components of the original matrix, whereas the last terms describe the high frequency components of A.

The first use of SVD in this work builds upon the work of Gonçalves et al. [11], in which the ultrafast dynamics of the methane cation excited by photoionization were computed. In order to create an initial state representative of the ones created in a typical experiment, in which the molecules are randomly oriented with respect to the direction of the electric field, it is more efficient computationally to fix the orientation of the molecule in the molecular frame and randomize the orientation of the exciting electric field with respect to the molecule, each direction leading to a different initial state. This means that in order to reproduce the results of experiments with molecules in a random orientation compared to the laboratory frame, it would be necessary to perform the dynamics on a large number of initial states produced from a random orientation of the electric field, and then study the average effect. Depending on the accuracy required to emulate the experimental conditions, a few thousands of those randomly oriented molecules might be necessary, thereby adding a large cost to the computations. Gonçalves et al. [11] reports another strategy to reduce the number of computations needed to construct a representative initial state for the photoionization of the methane cation: after having produced the set of randomly sampled initial states, the most significant features of this dataset are uncovered using SVD. They then proved that this reduces to only three non-zeros singular values and three associated singular vectors that, together, fully reproduce the features of the complete dataset. It is then sufficient to perform the dynamics on only the three singular vectors, instead of a few thousands of initial states, and then weigh the results obtained by the singular values to describe accurately the dynamics of a sample of randomly oriented molecules. This proves to yield good agreement with the experimental results of Marangos et al. [22].

In a similar spirit, the first part of my master thesis consisted in the study of the ultrafast Jahn-Teller effect in the methane cation, this time produced by strong field ionization. The initial state for the methane cation is again dependent on the orientation of the exciting electric field, and a similar need for an initial state representative of a sample of randomly oriented molecules is present. A similar strategy as in the case of the photoionization was thus performed. Contrary to photoionization, more than three singular values were required to fully describe the features of the dataset but taking only three proved to be sufficient to explain more than 99.5% of those features. The results obtained were then also in good agreement with the findings of Marangos et al. [22]. More information on this approach can be found in Blavier et al. [23].

The second use of SVD also relied on its property that singular vectors are obtained for both the column space and the row space of the matrix, providing information on the two different types of degrees of freedom described by the initial matrix. The amplitude vector **c** may be interpreted as a matrix connecting electronic and nuclear degrees of freedom, and SVD leads to a characterization of those two contributions separately, allowing to study the interplay between those degrees of freedom and even their entanglement. In this way, the SVD allows the computation of the Schmidt decomposition of the state of the system, a decomposition which provides a direct measure of the entanglement of a system through its rank. [24] The connection between SVD and the Schmidt decomposition, as well as the transformation of the amplitude vector in a suitable form is treated in more details in Blavier et al. [25].

Box 3. Entanglement

The concept of entanglement is another feature which is essential to quantum mechanics and often leads to non-intuitive effects. It is defined between two or more interacting systems on which it is possible, at least in theory, to make measurements separately. Entanglement arises from the fact that some (quantum) states from the overall system (A + B) cannot be described by the tensor product of states from the

subsystems (states from A and from B). One usual example is the Bell state for a system of two qbits $\frac{1}{\sqrt{2}}(|00\rangle+|11\rangle)$ which cannot, in any way, be expressed as the product of the states of one qbit ($|0\rangle$ or $|1\rangle$). The states that can be separated into different states of the subsystems are called separable states, whereas the others are entangled states. [26]

The problem of computing and characterizing the entanglement of a given quantum state is still an ongoing topic of investigation in quantum physics [27]. One simple criterion for bipartite system (a quantum system composed of two subsystems) consists of the Schmidt rank for the state, which is the minimum number of separable terms in the Schmidt decomposition of the state. For a separable state, the Schmidt rank is 1, whereas a Schmidt rank greater than or equal two 2 depicts an entangled state. This is this property of the Schmidt decomposition which allows to characterize the entanglement observed in molecular quantum dynamics [24, 26].

3. Results and discussion

3.1. Strong Isotope effect on the ultrafast Jahn-Teller Rearrangement of the methane cation

The first part of this work was devoted to the study of the Jahn-Teller rearrangement in the methane cation upon strong-field ionization, that is, the observed loss of symmetry of the CH_4 molecule when it is excited by a strong electric field, leading to high-harmonic generation. The harmonics produced can then be studied in order to better understand the quantum dynamics at play, a type of experiments call high-harmonic spectroscopy (HHS).

As said previously, this part built upon the previous work of Gonçalves et al. [11], who already investigated this effect in a molecular system excited by a short extreme UV optical pulse. The work began by the construction of the Hamiltonian operator associated with this system and was followed by the computation of initial states representative of the state produced by strong-field ionization of system to study the molecular dynamics.

This is where SVD crucially comes into play: as described earlier, SVD can be used to compute a low-rank approximation to any given matrix. A matrix composed of the amplitudes of 8000 random orientations of the exciting electric field was computed and then decomposed, which gave us access to the common features observed for all the different orientations, thereby reducing the task of computing the dynamics of 8000 initial states to only 3 which reproduce more than 99.5% of the features of the original matrix. This significant reduction in computational complexity of the problem allowed us to study the short-time dynamics of the Jahn-Teller rearrangement of CH_4^+, and characterize the isotope effect and the impact of the strength of the exciting electric field on the coherent dynamics.

For that purpose, two different values for the strength of the electric field were considered: a high value of 2×10^{14} W/cm^2, commonly used in high-harmonic spectroscopy experiments and referred to in the rest of this manuscript as strong field, and a lower value of 3.16×10^{13} W/cm^2, denoted as weak field. Computations were performed for both CH_4^+ and CD_4^+. The resulting electronic populations and electronic coherences are shown in figure 3.

As one can see, in both cases a coherent superposition of electronic states was created, with all electronic states being populated at the onset of the dynamics for both strengths of the electric field. Intuitively, a lower value of the strength led to a smaller population in the excited electronic states (D1 and D2) as the ionization potential of those electronic states was less modified by the weaker exciting electric field. The electronic populations are, however, similar between the two isotopomers of CH_4^+. A clearer

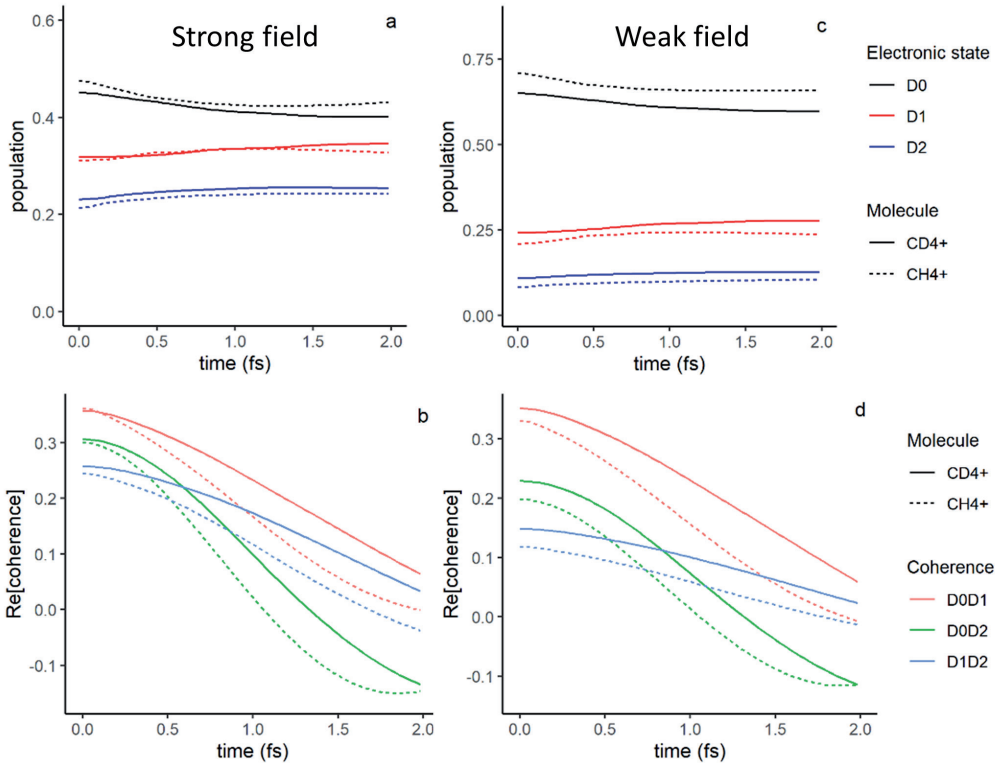

Figure 3: Electronic populations (a, c) and real part of the electronic coherences (b, d) at short times, for respectively the strong field (left) and the weak field (right)

difference can be observed in the real part of the electronic coherences. The oscillations of the coherence are slower in the case of CD_4^+ as the highest mass of the molecular system leads to a slower motion of the wave packets on the electronic states. The electronic coherences therefore prove to be more sensitive to the isotope effect than the populations.

One of the aims of this study was to understand the isotope effect observed experimentally in the yield in harmonics obtained during a HHS experiment, as reported by Marangos et al. [22] This can be assessed theoretically by studying the evolution of the autocorrelation function $|C(t)|^2=\psi(0)^*\psi(t)$, which has been shown to be proportional to this yield in harmonics [29].

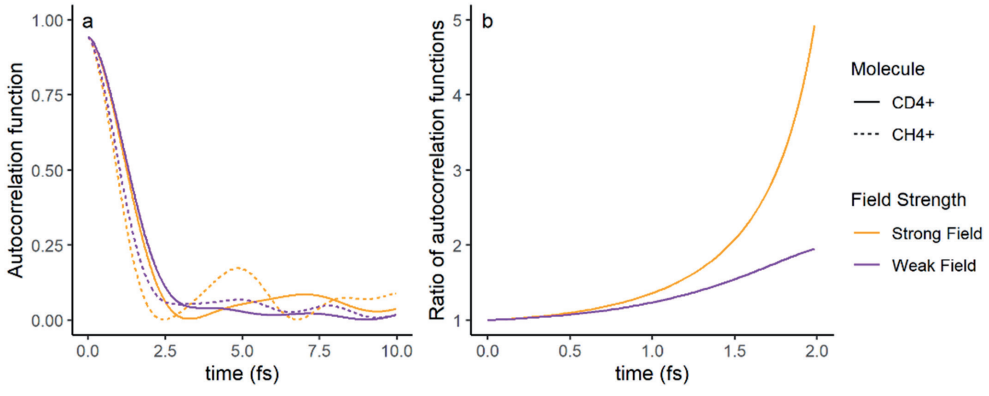

Figure 4: Autocorrelation function (a) and ratio of the autocorrelation functions (b) between CD_4^+ and CH_4^+

The ratio in the autocorrelation functions for CH_4^+ and CD_4^+ can therefore be compared with the ratio of the yields in harmonics obtained. As shown in figure 4, this ratio has been found to be approximately 2.4 at 1.6 fs in the case of the strong field, which is in agreement with the values found experimentally.

One crucial remark to make on this result is that the isotope effect observed in the ratio of the autocorrelation functions is greater than the one simply induced by the difference in mass of the two isotopomers. It mainly arises from the impact of the non-adiabatic couplings between the D_2 state and the others, leading to different dynamics at short times. This highlights the effects that non-adiabatic couplings can have on molecular quantum dynamics.

More information on this work can be found in the article Blavier et al. [23], as the aim of this section was to illustrate the handiness of SVD to reduce the computational cost of the quantum dynamics. Another aspect of this usefulness will now be exemplified with the characterization of the entanglement between electronic and nuclear degrees of freedom in the LiH molecule.

3.2. Analysis of the entanglement within the LiH molecule

To understand the insights that SVD can provide on the interactions between electronic and nuclear degrees of freedom, the choice was made to consider a simpler system than the methane cation, namely lithium hydride (LiH). This molecule is a linear diatomic molecule with a single nuclear degree of freedom, the internuclear distance R. The photoexcitation of this molecule by a few fs deep-UV pulse was then computed, a photoexcitation which led to the creation of a coherent superposition of electronic states and thus to coherent nuclear dynamics. Among the six excited electronic states considered in the dynamics, the most populated by the pulse were the Σ_2 and Σ_4 states. Of all the electronic states that were resonant with the optical pulse, those two indeed possess a stronger transition dipole moment, explaining the difference in population shown in figure 5.

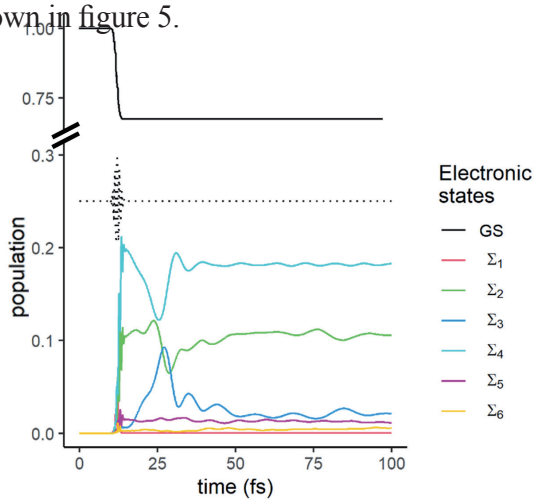

Figure 5: Population of the Σ_2, Σ_3 and Σ_4 electronic states through time. Note the break in the y axis separating the population of the ground state from the rest. The exciting optical pulse is represented as a black dotted line. Reproduced from Ref. [25] with permission from the PCCP Owner Societies.

As one can see from figure 5, the , and electronic states exhibit the strongest population transfers through time and are the most interesting for the analysis of the electronic coherence. This is because of the strong non-adiabatic couplings that take place between those three electronic states.

The first parameter given to us by the singular value decomposition that we can analyse is the singular values. Drawing from the analogy between the Schmidt decomposition of a quantum system and the SVD, we can infer that if only one singular value is needed for the description of our molecular system at a given time, the system is in a separable state at that time. The evolution through time of the singular values is represented in figure 6.

As one can see, before the onset of the exciting optical pulse, the system lies in a separable state described only by one singular value, which is intuitive as all the electronic wave packet is located on the ground state of the molecule. As soon as the optical pulse creates a coherent superposition of electronic states, at least two singular values are required to describe the state of the system. The coherent excitation of the pulse thus leads to an increase of the entanglement of the state of the molecular

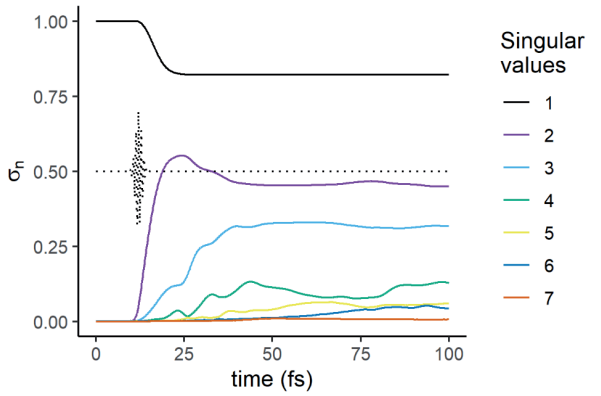

Figure 6: Evolution through time of the singular values. The exciting optical pulse is represented in black. Reproduced from Ref. [25] with permission from the PCCP Owner Societies.

system. An important note has to be made here: the creation of a coherent superposition of electronic states is not a sufficient condition for an increase in the entanglement. Indeed, if all the electronic states possessed the same potential energy surfaces, and thus the same gradient, the motion of the wave packets on each electronic state of the superposition would be identical, leading to a separable state as only one nuclear state is required to explain the motion of all the electronic wave packets.

The previous remark introduces the importance of the difference in the gradients on different electronic states to produce an increase in the entanglement of the system. It also allows us to understand the dynamics of the singular values in figure 6. Indeed, at the maximum of the pulse, where the amplitude transfers between electronic states is the highest, the system still lies in a separable state. This is because the wave packets did not have any time to move and are still all localized in the Franck-Condon region of the molecule. As soon as the wave packets begin to move on their respective potential energy surfaces, the entanglement of the state increases. Similarly, the appearance of new singular values in the description of the state of the system is correlated with the differing motions of wave packets on different potential energy surfaces.

In addition to the differing gradients of the electronic states, non-adiabatic couplings (NAC) also play a role in the evolution of the entanglement of the system. Their role can be highlighted by comparing the previous computational simulation with a simulation excluding the impact of NACs. A comparison of the evolution through time of the singular values for both the original computation and the one without NACs is shown in figure 7. This figure provides further insight in the time-evolution of the third and fourth singular values, as the moment of the onset of their rise changes strongly between the two simulations. It suggests that the effect of NACs on the entanglement of the state of the molecule is the strongest between 15 and 25 fs, and after that the main effect comes from the aforementioned difference in the gradients of the potential energy surfaces of each electronic state.

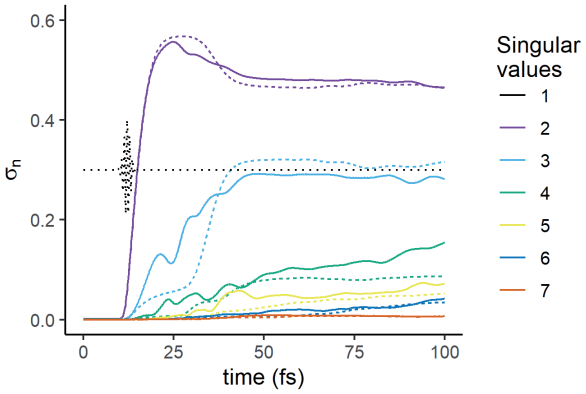

Figure 7 : Evolution through time of the singular values for a simulation with non-adiabatic couplings (full lines) and without (dashed lines). The exciting optical pulse is represented in black. Reproduced from Ref. [25] with permission from the PCCP Owner Societies.

One way to verify this conclusion on the importance of the gradients of the electronic states is to study the singular vectors, which constitute an orthonormal basis for the states of the system, respectively for the nuclear degrees of freedom in the case of the left singular vectors and the electronic degrees of freedom for the right singular vectors. The singular vectors corresponding to the first four states of the SVD are shown in figure 8 and figure 9.

These two figures show the left singular vectors associated with each singular value, which represent a nuclear state and thus a localization on the grid, and the right singular vectors displaying an electronic state and thus a sort of “electronic composition” of the state in the SVD considered.

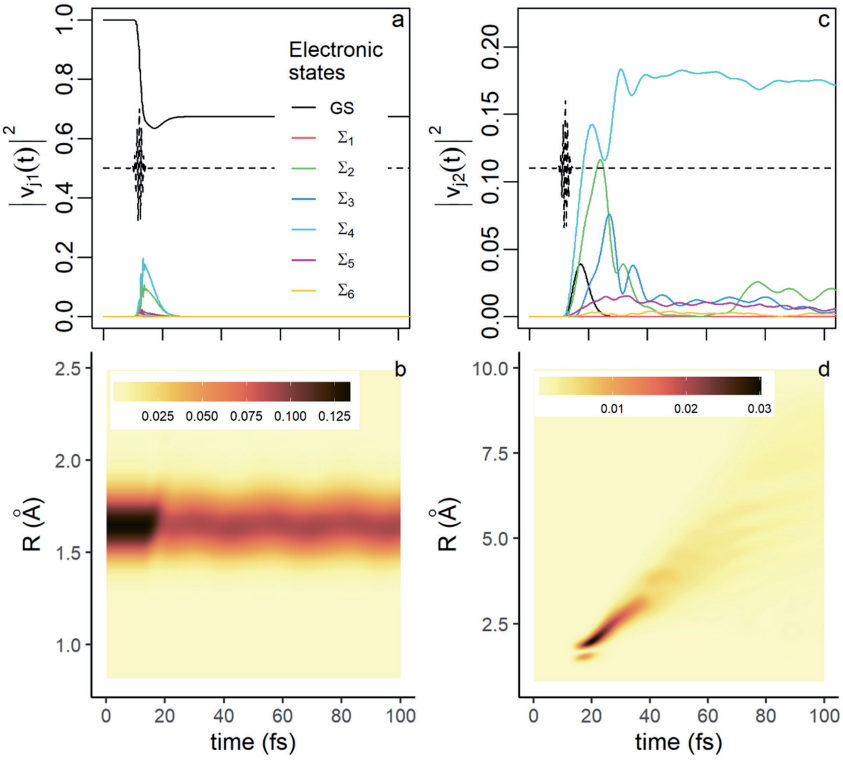

Figure 8: Left and right singular vectors associated with the first and second singular values. They are weighted by the singular values in order to better describe their importance for the description of the state of the system. Reproduced from Ref. [25] with permission from the PCCP Owner Societies.

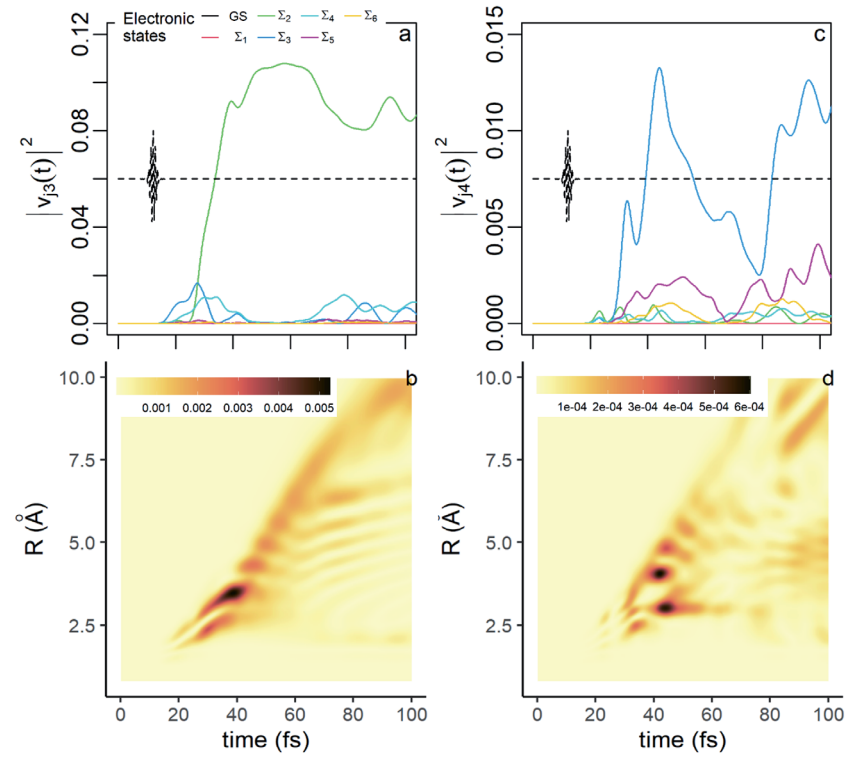

Figure 9: Left and right singular vectors associated with the third and fourth singular values. They are weighted by the singular values in order to better describe their importance for the description of the state of the system. Reproduced from Ref. [25] with permission from the PCCP Owner Societies.

This information confirms and improves the previous analysis that was performed on the basis of the singular values alone. The figures 8a and 8b show that the state associated with the first singular value is mostly composed of the ground state of the molecule and localized in the Franck-Condon region, except during the interaction with the optical pulse where a part of this state is localized on the excited electronic states, reflecting the previous note on the increase of the second singular value after the peak of the exciting pulse.

The subsequent singular vectors allow us to understand the appearance of the third singular value. The electronic composition of the second singular state (figure 8c) shows that it corresponds initially (just after the pulse) to a state with contributions of both the Σ_4 and Σ_2 ; electronic states, but then quickly loses its Σ_2 component as the wave packets of these two electronic states exhibit different motions on their respective potential energy surfaces. This timing is consistent with the rise of the third singular value, mainly localized on the Σ_2 electronic state (see figure 9a). The left singular vectors indicate that the wave packets corresponding to the second, third and fourth singular values all display a dissociative behaviour, their trajectory escaping from the Franck-Condon region of the system.

This constitutes a short overview of how SVD allows for some insight into the evolution of the entanglement in the simple molecular system which is LiH. Further information can be found in the article Blavier et al. [25].

4. Conclusion

The complex phenomena and behaviours arising from the interaction of matter with ultrafast optical pulses is at the same time one of the strongest motivations for the study of attosecond chemistry, and also the main reason for which such research is far from being straightforward. The purely coherent quantum dynamics created by the significant energy bandwidth of the attopulses used force us to perform fully quantum dynamics on molecular systems, which remains for the moment a computationally intensive endeavour. Those issues constitute a significant bottleneck for the in-depth study of experimental data and the rationalization of the interactions between ultrashort pulses and molecules, which could enable a first step towards preparative or synthetic attochemistry.

These technical considerations aside, the study of attochemistry is also hampered, both experimentally and theoretically, by the amount and the complexity of the data produced which tremendously complicates their analysis, leading to another restrain in our ability to more finely understand attochemical phenomena.

Therefore, any technique which might accelerate or simplify either theoretical computations or data analysis and could improve our understanding of the coherent effects at play is important. As discussed in this article, singular value decomposition seems to be a valuable candidate for both considerations. It allowed us to reduce tremendously the number of initial states to consider to describe the random orientations of the molecules in the dynamics of the ultrafast Jahn-Teller rearrangement of the methane cation, leading to a significant decrease in the computational work required to model the evolution of the system, while keeping a good agreement with experimental results. Used as a method to compute the Schmidt decomposition of the wavefunction in LiH, it allowed a characterization of the time-evolution of the entanglement of the state of the system, providing novel insight in the interplay of nuclear and electronic degrees of freedom in molecular quantum dynamics.

It is almost certain that the singular value decomposition and similar algebraic decomposition will continue to find new uses in the analysis of ultrafast coherent molecular dynamics, as their handiness has now evaded the field of the statistics and linear algebra to enable new insights and provide solutions to problems in other fields.

Acknowledgements

This work was supported by the Fonds National de la Recherche Scientifique (Belgium), F.R.S.-FNRS research grants # T.0205.20. Computational resources have been provided by the Consortium des Equipements de Calcul Intensif (CECI), funded by the F.R.S.- FNRS under Grant # 2.5020.11. Support of the COST action Attochem (CA18222) is acknowledged. Support of the FRIA is also acknowledged.

The author would like to greatly thank Pr. Françoise Remacle, without whom all this work would not have been possible. Her review on the present manuscript proved to be instrumental to its quality. The author would also like to thank Kyde Bellon for his kind proofreading of this manuscript.

References

[1] Balzani, V. Photochemistry and Photophysics: Concepts, Research, Applications. **2014**, 502.

[2] Corkum, P. B.; Krausz, F. Attosecond Science. *Nat. Phys.* **2007**, *3* (6), 381–387.

[3] Remacle, F.; Levine, R. D. An Electronic Time Scale in Chemistry. *Proc. Natl. Acad. Sci.* **2006**, *103* (18), 6793–6798.

[4] Kling, M. F.; Vrakking, M. J. J. Attosecond Electron Dynamics. *Annu. Rev. Phys. Chem.* **2008**, *59* (1), 463–492.

[5] F. Lépine, M. Y. Ivanov, M. J. Vrakking, J. Nat. Photonics 2014, 8 (3), 195–204.

[6] Nisoli, M.; Decleva, P.; Calegari, F.; Palacios, A.; Martín, F. Attosecond Electron Dynamics in Molecules. *Chem. Rev.* **2017**, *117* (16), 10760–10825.

[7] Zewail, A. H. Femtochemistry: Atomic-Scale Dynamics of the Chemical Bond. *J. Phys. Chem. A* **2000**, *104* (24), 5660–5694.

[8] Reiter, S.; Keefer, D.; Vivie-Riedle, R. Exact Quantum Dynamics (Wave Packets) in Reduced Dimensionality. In *Quantum Chemistry and Dynamics of Excited States*; González, L., Lindh, R., Eds.; Wiley, 2020; pp 355–381.

[9] Cohen-Tannoudji, C.; Diu, B.; Laloë, F. *Mecanique Quantique*; Collection Enseignement des sciences, 16; Hermann: Paris, 1973.

[10] Levine, I. N. *Quantum Chemistry*, Seventh edition.; Pearson: Boston, 2014.

[11] C. E. M. Gonçalves, R. D. Levine, F. Remacle, Phys. Chem. Chem. Phys. 2021, 10.1039.D1CP01029H.

[12] Ajay, J. S.; Komarova, K. G.; Van Den Wildenberg, S.; Remacle, F.; Levine, R. D. CHAPTER 9. Attophotochemistry: Coherent Electronic Dynamics and Nuclear Motion. In *Theoretical and Computational Chemistry Series*; Vrakking, M. J. J., Lepine, F., Eds.; Royal Society of Chemistry: Cambridge, 2018; pp 308–347.

[13] Born, M.; Oppenheimer, R. Zur Quantentheorie der Molekeln. *Ann. Phys.* **1927**, *389* (20), 457–484.

[14] Matsika, S. Electronic Structure Methods for the Description of Nonadiabatic Effects and Conical Intersections. *Chem. Rev.* **2021**, *121* (15), 9407–9449.

[15] van den Wildenberg, S.; Mignolet, B.; Levine, R. D.; Remacle, F. Temporal and Spatially Resolved Imaging of the Correlated Nuclear-Electronic Dynamics and of the Ionized Photoelectron in a Coherently Electronically Highly Excited Vibrating LiH Molecule. *J. Chem. Phys.* **2019**, *151* (13), 134310.

[16] Shiner, A. D.; Schmidt, B. E.; Trallero-Herrero, C.; Wörner, H. J.; Patchkovskii, S.; Corkum, P. B.; Kieffer, J.-C.; Légaré, F.; Villeneuve, D. M. Probing Collective MultiElectron Dynamics in Xenon with High-Harmonic Spectroscopy. *Nat. Phys.* **2011**, *7* (6), 464–467.

[17] Abdi, H.; Williams, L. J. Principal Component Analysis: Principal Component Analysis.

Wiley Interdiscip. Rev. Comput. Stat. 2010, 2 (4), 433–459.

[18] Andrews, H.; Patterson, C. Singular Value Decomposition (SVD) Image Coding. *IEEE Trans. Commun.* **1976**, *24* (4), 425–432.

[19] Alter, O.; Brown, P. O.; Botstein, D. Singular Value Decomposition for Genome-Wide Expression Data Processing and Modeling. *Proc. Natl. Acad. Sci.* **2000**, *97* (18), 10101– 10106.

[20] Remacle, F.; Kravchenko-Balasha, N.; Levitzki, A.; Levine, R. D. Information-Theoretic Analysis of Phenotype Changes in Early Stages of Carcinogenesis. *Proc. Natl. Acad. Sci.* **2010**, *107* (22), 10324–10329.

[21] H. Abdi, in 'Encyclopedia of measurement and statistics', Eds. N. J. Salkind,
K. Rasmussen, Thousand Oaks, Calif, 2007, p. 14.

[22]. Marangos, J. P.; Baker, S.; Kajumba, N.; Robinson, J. S.; Tisch, J. W. G.; Torres, R. Dynamic Imaging of Molecules Using High Order Harmonic Generation. *Phys Chem Chem Phys* **2008**, *10* (1), 35–48.

[23] M. Blavier, K. Komarova, C. E. Gonçalves, R. D. Levine, F. Remacle, J. Phys. Chem. A 2021, 125 (43), 9495–9507.

[24] A. Ekert, P. L. Knight, Am. J. Phys. 1995, 63 (5), 415–423.

[25] M. Blavier, R. D. Levine, F. Remacle, Phys. Chem. Chem. Phys. 2022, 24, 17516-17525.

[26] Nielsen, M. A.; Chuang, I. L. *Quantum Computation and Quantum Information*, 10th anniversary ed.; Cambridge University Press: Cambridge ; New York, 2010.

[27] Horodecki, R.; Horodecki, P.; Horodecki, M.; Horodecki, K. Quantum Entanglement. *Rev. Mod. Phys.* **2009**, *81* (2), 865–942.

[28] Zhao, S.-F.; Xu, J.; Jin, C.; Le, A.-T.; Lin, C. D. Effect of Orbital Symmetry on the Orientation Dependence of Strong Field Tunnelling Ionization of Nonlinear Polyatomic Molecules. *J. Phys. B At. Mol. Opt. Phys.* **2011**, *44* (3), 035601.

[29] Lein, M. Attosecond Probing of Vibrational Dynamics with High-Harmonic Generation. *Phys. Rev. Lett.* **2005**, *94* (5), 053004.